US Army Research Laboratory

Compression of Ultrafast Laser Beams

by Stephen Roberson and Paul Pellegrino

NOTICES

Disclaimers

The findings in this report are not to be construed as an official Department of the Army position unless so designated by other authorized documents.

Citation of manufacturer's or trade names does not constitute an official endorsement or approval of the use thereof.

Destroy this report when it is no longer needed. Do not return it to the originator.

US Army Research Laboratory

Compression of Ultrafast Laser Beams

by Stephen Roberson
EOIR Technologies, Springfield, VA

Paul Pellegrino
Sensors and Electron Devices Directorate, ARL

REPORT DOCUMENTATION PAGE				*Form Approved* *OMB No. 0704-0188*
Public reporting burden for this collection of information is estimated to average 1 hour per response, including the time for reviewing instructions, searching existing data sources, gathering and maintaining the data needed, and completing and reviewing the collection information. Send comments regarding this burden estimate or any other aspect of this collection of information, including suggestions for reducing the burden, to Department of Defense, Washington Headquarters Services, Directorate for Information Operations and Reports (0704-0188), 1215 Jefferson Davis Highway, Suite 1204, Arlington, VA 22202-4302. Respondents should be aware that notwithstanding any other provision of law, no person shall be subject to any penalty for failing to comply with a collection of information if it does not display a currently valid OMB control number. **PLEASE DO NOT RETURN YOUR FORM TO THE ABOVE ADDRESS.**				
1. REPORT DATE *(DD-MM-YYYY)* March 2016	**2. REPORT TYPE** Final		**3. DATES COVERED (From - To)** 1–31 December 2014	
4. TITLE AND SUBTITLE Compression of Ultrafast Laser Beams			**5a. CONTRACT NUMBER**	
			5b. GRANT NUMBER	
			5c. PROGRAM ELEMENT NUMBER	
6. AUTHOR(S) Stephen Roberson and Paul Pellegrino			**5d. PROJECT NUMBER**	
			5e. TASK NUMBER	
			5f. WORK UNIT NUMBER	
7. PERFORMING ORGANIZATION NAME(S) AND ADDRESS(ES) US Army Research Laboratory ATTN: RDRL-SEE-E 2800 Powder Mill Road Adelphi, MD 20783-1138			**8. PERFORMING ORGANIZATION REPORT NUMBER** ARL-TR-7640	
9. SPONSORING/MONITORING AGENCY NAME(S) AND ADDRESS(ES)			**10. SPONSOR/MONITOR'S ACRONYM(S)**	
			11. SPONSOR/MONITOR'S REPORT NUMBER(S)	
12. DISTRIBUTION/AVAILABILITY STATEMENT Approved for public release; distribution is unlimited.				
13. SUPPLEMENTARY NOTES				
14. ABSTRACT Compression of ultrafast laser pulses is critical to obtain optimal results from many experiments that use a femtosecond laser system. However, as the pulse lengths decrease and peak pulse power increases, pulse compression using static elements such as prisms may not be sufficient to completely compress the laser pulse. This report details the complete construction of a spatial light modulator (SLM)-based 4*f* Fourier pulse shaper that is used in femtosecond laser pulse compression. First, the theory behind compression of femtosecond lasers is covered and initial pulse compression efforts using static elements are discussed. Next, all aspects of the SLM pulse shaper construction are covered, including part selection, alignment, and calibration curve determination. This technical report also discusses the theory, construction, and evaluation of 2 separate algorithms, a modified genetic algorithm and the multiphoton intrapulse interference phase scan (MIIPS) algorithm, used to optimally compress the femtosecond laser pulses using the pulse shaper. The efficacy of these 2 algorithms when used for pulse compression was evaluated, and it was found that the MIIPS algorithm was superior to the genetic algorithm for pulse compression.				
15. SUBJECT TERMS ultrafast lasers, pulse compression, genetic algorithm, MIIPS algorithm, pulse shaping, pulse shaper construction				
16. SECURITY CLASSIFICATION OF:			**17. LIMITATION OF ABSTRACT**	**18. NUMBER OF PAGES**	**19a. NAME OF RESPONSIBLE PERSON** Stephen Roberson
a. REPORT Unclassified	**b. ABSTRACT** Unclassified	**c. THIS PAGE** Unclassified	UU	34	**19b. TELEPHONE NUMBER (Include area code)** 301-394-1347

Contents

List of Figures

1. Introduction

A pulsed laser is normally considered an ultrafast pulsed laser when the pulse duration of that laser is in the realm of picoseconds and below.[1] Ultrashort laser pulses deliver a very high peak power to their targets because of their short durations. There are many favorable qualities associated with an ultrafast pulsed laser beam. One positive feature is their very short pulse time spans and the resulting temporal resolution. A femtosecond pulsed laser allows for ultrafast laser excitation as well as measurements of physical systems that may not be possible with lasers with longer pulse widths. Also, the high peak power from an ultrafast pulsed laser beam allows the user to take advantage of nonlinear optical processes, such as sum and difference frequency generation and supercontinuum generation, more easily than with other types of lasers. Another aspect of ultrashort laser pulses is that the high peak power from ultrafast pulsed lasers allows for femtosecond laser-induced breakdown spectroscopy and more precise laser machining. Additionally, because of the Heisenberg uncertainty principle, ultrafast lasers contain multiple coherent wavelengths of light. As the laser pulse is shortened, the bandwidth of the laser broadens. This broadband feature of an ultrafast laser beam is widely used in research, including quantum controls of molecular properties.

The equation describing the propagation of light as a plane wave is

$$E = E_0 \exp\left[i\left(\vec{k} \cdot \vec{r} - \phi(t)\right)\right], \tag{1}$$

where k is the propagation constant defined as $\left|\vec{k}\right| = \frac{2\pi}{\lambda} = \frac{\omega}{c}$ and $\phi(t)$ is the temporal phase of the plane wave.[2] One can create an expression for a pulsed laser pulse by multiplying the expression for a plane wave by a Gaussian function. The temporal aspects of a Gaussian laser pulse can be described mathematically as

$$E(t) = E_0 \exp[-\alpha t^2] \exp[-i\phi(t)], \tag{2}$$

where E_0 is the amplitude of the pulse, and $\alpha^{-1/2}$ relates to the pulse duration. From this expression, it is possible to calculate the frequency representation of the laser pulse $\varepsilon(\omega)$ by taking the Fourier transform of $E(t)$:

$$\varepsilon(\omega) = \frac{1}{2\pi} \int_{-\infty}^{\infty} E(t)\exp[i\omega t]dt. \tag{3}$$

If $\phi(t)$ is either a constant or a linear function of t, such as $\phi(t) = \omega_0 t$, then the phase does not have any bearing on the overall temporal pulse characteristics (i.e., the pulse length is unchanged). A laser pulse that has a constant or linear phase is known as a transform limited beam. However, if $\phi(t)$ is a second-order function or higher, the pulse length and other characteristics are affected. An ultrashort pulse

with a nonlinear temporal phase profile is also known as a chirped pulse. Normally we measure the intensity $I(t)$ and spectrum $S(\omega)$ of a laser pulse. The intensity $I(t)$ of a laser pulse is described mathematically by $I(t) = |E(t)|^2$, and the spectrum of a laser pulse $S(\omega)$ can be described mathematically with $S(\omega) = |\varepsilon(\omega)|^2$. The intensity and the spectrum of a laser pulse are what is commonly measured when dealing with light.

The ideal temporal state of an ultrafast pulsed laser beam is a transform-limited laser beam. When an ultrafast laser beam travels through the air or through other materials, it experiences group velocity dispersion (GVD) because it comprises multiple wavelengths. Dispersion is the effect of the air or other refractive medium on the optical properties of a laser pulse. The light from an ultrafast laser beam consisting of a multitude of wavelengths moves through the air at different velocities because of the refractive index of the air. To describe dispersion mathematically, one would start with the Fourier transform of a Gaussian pulse with a linear phase at the origin:

$$\varepsilon_0(\omega) = \exp\left[\frac{-(\omega-\omega_0)^2}{4\alpha}\right]. \tag{4}$$

As that pulse moves a distance x from the origin, the equation becomes

$$\varepsilon(\omega, x) = \varepsilon_0(\omega)\exp[-ik(\omega)x] \tag{5}$$

because of the spatial component of the equation. The propagation of the laser beam through a transparent medium is now frequency dependent as it moves from the origin. This spread of velocities due to the constituent wavelengths of the laser pulse means that the wavelengths of the pulse will arrive at a desired point at different times, resulting in a temporally longer laser pulse. A transform-limited laser beam is ideal for ultrafast laser studies because all the constituent wavelengths arrive at a desired point in time. It is critical when working with an ultrafast laser beam to be able to control the dispersion the beam experiences when it interfaces with refractive materials.

The ultrafast laser system in our laboratory consists of a Micra oscillator that outputs pulses on the order of a few nanojoules per pulse at an 81-MHz repetition rate and a Coherent Legend Elite that outputs a 40-fs Gaussian pulse at a kilohertz repetition rate with a pulse energy of 3 mJ/pulse. The pulse diameter of this beam is approximately 8 mm. Since the laser pulse duration cannot be measured with conventional electronic means, we used both a home-built FROG[3] and a GRENOUILLE[4] purchased from Swamp Optics to verify that the beam is essentially transform limited when it exits the Legend Elite.

2. Second Harmonic Generation

Because of the extremely short duration of the laser pulses being measured in this experimental setup, conventional methods of measuring laser pulse duration, such as using a photodiode and oscilloscope, cannot be used. Second harmonic generation (SHG) is a type of nonlinear phenomenon that occurs when 2 lasers of the same wavelength combine to form one photon with twice the energy of one of the original photons when propagating through a suitable nonlinear material. SHG of a laser pulse is a nonlinear optical effect used frequently in ultrafast optics to double the frequency of a laser beam for a wide variety of applications.[5] SHG can be expressed mathematically by starting with our broadband laser pulse:

$$|\epsilon(\omega + \Omega)| \exp[i\phi(\omega + \Omega)] , \qquad (6)$$

where $|\epsilon(\omega + \Omega)|$ is the amplitude of the pulse, $\exp[i\phi(\omega + \Omega)]$ is the phase of the pulse, and $(\omega + \Omega)$ is the detuning of the pulse due to the pulse's broadband nature. Under single cycle approximation, the second harmonic signal, $S(2\omega)$, can be written as an integral:

$$S(2\omega) = \left| \int d\Omega |\epsilon(\omega + \Omega)| |\epsilon(\omega - \Omega)| \exp\left[i\left(\varphi(\omega + \Omega)\right)\right] \exp\left[i\left(\varphi(\omega - \Omega)\right)\right] \right|^2. \quad (7)$$

Measuring extremely short-duration pulses requires interferometric methods of measuring pulse duration, such as autocorrelation. In autocorrelation, the initial pulse is split into 2 pieces: a reference pulse and a delay pulse. The delay pulse moves through an arm that changes the path length of the beam while the reference pulse does not. Those 2 pulses are recombined in an appropriate nonlinear material to create a second harmonic signal from the 2 beams. The creation of SHG light would require that the 2 photons with the required wavelengths are in the nonlinear material at the same time. As the pulse in the delay line is moved in time with respect to the other, a second harmonic signal due to their temporal overlap can be observed. The intensity of the resultant second harmonic signal, also known as the autocorrelation signal A_{SHG}, is given by

$$A_{SHG}(\tau) = \int_{-\infty}^{\infty} I(t)I(t - \tau)dt. \qquad (8)$$

The knowledge of the amount of delay given to the delay pulse combined with the strength of the resulting SHG signal due to that delay allows for calculation of the pulse duration.

In addition to using SHG to determine the pulse duration of an ultrafast pulse, it can be used to determine the phase characteristics of a laser pulse, namely the degree of dispersion of a laser pulse. The expression for the intensity of the second harmonic signal I generated in an appropriate nonlinear material of length L is

$$I(L,t) = \frac{c\mu_0\omega_0^2}{4}|P|^2L^2 sinc^2\left(\frac{\Delta kL}{2}\right), \tag{9}$$

where P refers to the polarization, L is the length of the material used to generate the second harmonic signal, ω_0 is the output frequency that is related to the output wavelength, Δk is a quantity related to the dispersion of the light, c is the speed of light, μ_0 is the magnetic permeability of free space, and

$$\text{sinc}(\Delta kL/2) = \frac{\sin(\Delta kL/2)}{\Delta kL/2}. \tag{10}$$

The intensity of the SHG signal is dependent in part on the thickness of the crystal. However, as the crystal length increases, sinc($\Delta kL/2$) becomes a constant value no matter the degree of dispersion in the beam creating the SHG signal. Additionally, as the laser beam moves through a crystal to create an SHG signal, the beam experiences dispersion from the crystal. This additional dispersion would result in an inaccurate measurement of pulse duration, so it is important that the crystal is thin to minimize the dispersion imposed on the incoming laser beam.

The function sinc($\Delta kL/2$) is maximized when $\Delta kL/2$ is minimized, which occurs when $\Delta k = 0$. This condition is indicative of a transform-limited beam. Therefore, the thinner the crystal, the closer to transform limited the pulse must be in order to generate a strong SHG signal.

3.   Prism Compressor

A number of devices can be used to counteract dispersion and produce a transform-limited laser pulse. One widely used method of removing linear dispersion from a laser pulse is to use a prism compressor. A prism compressor works by passing laser light through an optically transparent set of prisms to remove GVD from a laser pulse.[6] The laser pulse is refracted through a prism at the Brewster angle and dispersed into its constituent wavelengths. It is then refracted through another identical but antiparallel prism that is separated by the distance necessary to compensate for the positive dispersion and produce a transform-limited pulse. The light passes through another identical prism, which puts the pulse back together, and then a final antiparallel prism to the third prism. When the laser beam passes through the prism compressor, it experiences negative GVD, eliminating the positive GVD the pulse receives from traveling through the air or other refractive medium. The total length of the laser pulse through the prism compressor is the length needed to generate the negative GVD necessary to counter the positive dispersion the laser beam received from going through the air and other refractive materials. This 4-prism compressor setup is simplified by placing a mirror after the second prism in a 2-prism compressor setup to reflect the beam back through the

2-prism setup, or by using a retroreflector and a roof mirror to reflect the laser pulse through a prism 4 times as seen in a single-prism compressor setup.[7]

We constructed a single-prism compressor (Fig. 1) to compress the broadband white light pulse needed to do multiplex coherent anti-Stokes Raman spectroscopy (MCARS).[8] With MCARS, we use a thin probe pulse in conjunction with a broad white light pump pulse to obtain vibration Raman spectra on a millisecond time scale. The vibrational spectra are optimized when the broad white light pulse is well compressed. In the laboratory, a white light laser pulse is generated by focusing a small portion of the femtosecond laser pulse in a random cut sapphire plate and allowing the subsequent self-phase modulation to create a white light laser beam with a bandwidth of over 100 nm. Figure 2 shows the spectrum of the white light generated with the sapphire plate combined with the probe pulse. This white light is used to obtain a CARS signal of the target. The strength of the CARS signal is dependent on the intensity of the laser pulse, so the CARS signal is optimized with the compressed white light laser pulse. To compress this white light, we built 2 different prism compressors: a 2-prism compressor and a single-prism compressor. One advantage of the single-prism compressor is that alignment is needed for one prism instead of two. The single-prism compressor also reduces the amount of table space needed to create the length necessary for compression. Figure 3 shows an example of the FROG spectrum before and after the beam is compressed with the pulse compressor. The white light laser beam started with a pulse width of 80 fs before compression and ended with a pulse length of around 25 fs.
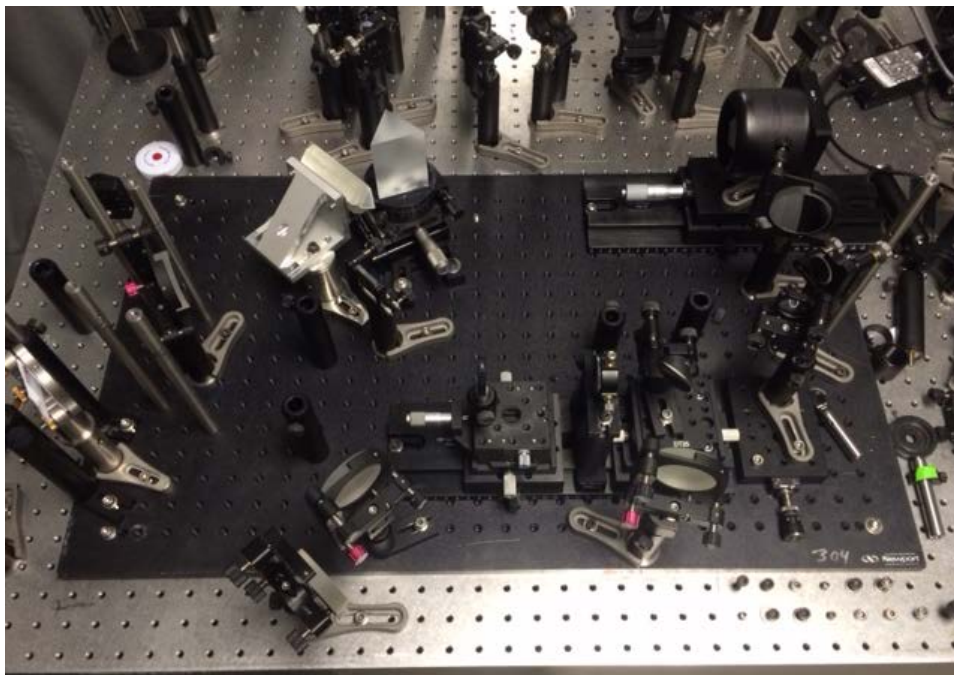

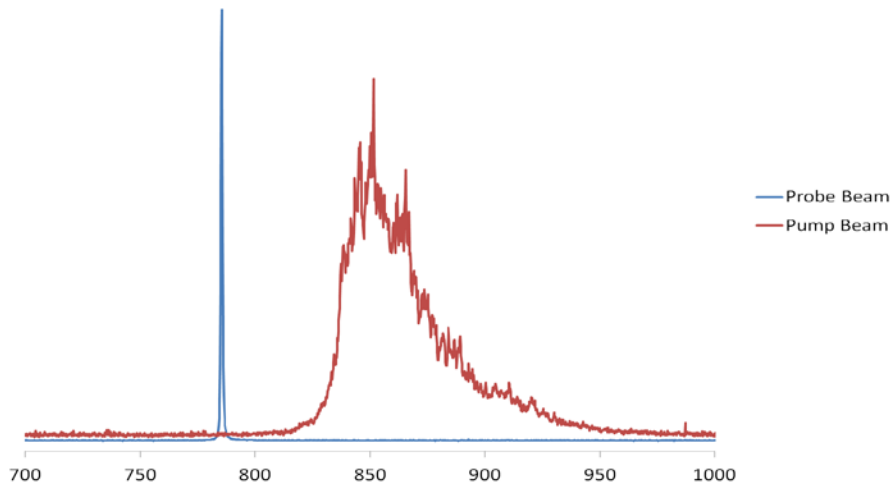**Fig. 1   Single prism pulse compressor**
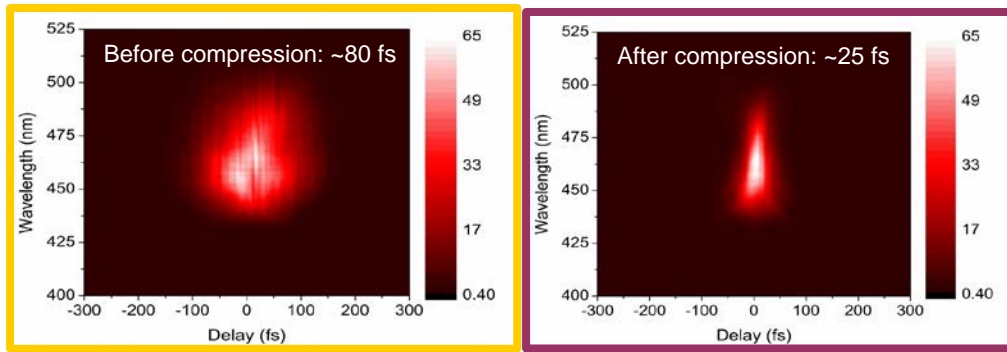
Fig. 2   Pump and probe spectra

Fig. 3   Before and after FROG spectra from the pulse compression

The effectiveness of these compressors in compressing the white light is limited as the laser pulses become shorter and the bandwidths associated with them become larger. The index of refraction of most materials is not uniform as a function of wavelength, so a pulsed beam with a large bandwidth will not be uniformly compressed. In our research, the theoretical limit of compression of the white light beam seen in Fig. 2 is considerably shorter than 25 fs, and our setup has not yet been able to compress the pulse with the prism compressor below 25 fs. Additionally, prism-based pulse compressors cannot handle anything other than a linear dispersion. As the laser pulse becomes shorter and more powerful, nonlinear dispersion effects on the laser beam become more of a concern.

4. Programmable Pulse Shaper

A pulse shaper is a powerful tool that can be used for different types of pulse manipulation, including pulse compression. All pulse shapers have a device that alters various pulse characteristics, such as the transmission, the phase, the polarization, or a combination of these characteristics. Originally, fixed elements using microlithographic patterning techniques were used as a mask for the beam. Some pulse shapers use elements that can be programmed to dynamically modify the light pulse. More recent pulse shapers use programmable elements like acousto-optic modulators, deformable mirrors, and spatial light modulators to modify the pulse characteristics of the dispersed beam.

We built a Fourier-transform $4f$ optical pulse shaper. In this pulse shaper, the femtosecond pulse is dispersed into its constituent wavelengths using a grating or a prism and that dispersed light travels a distance f and is collected with a focusing element, usually a lens or a mirror, where the f is equal to the focal length of the focusing element.[1] The light travels a distance f from the focusing element and encounters the device that is used to make changes to the pulse characteristics. Once the changes are made to the pulse, it travels another distance f to another focusing element, which focuses the beam back to its original dimensions. At that focal length f, the beam encounters another dispersive element where the beam wavelengths are recombined. As seen in Fig. 4, the distance from the grating to the focusing element must be the same distance from the focusing element to the pulse modification device, which is the focal length of the focusing element. These distances are maintained from the pulse modification device to the focusing element and from the focusing element back to the grating.
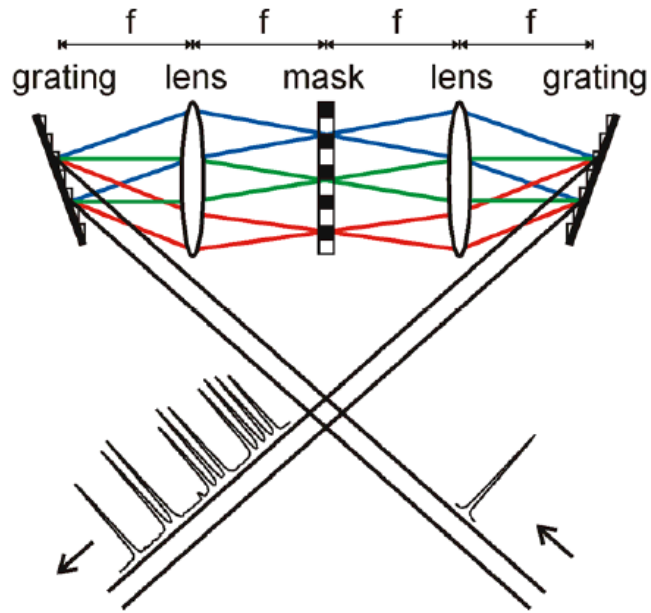
Fig. 4 Basic layout for a 4f Fourier transform pulse shaper. (Image used with permission from Vaughn[9].)

The schematic used as a basis for the pulse shaper we constructed is seen in Fig. 5.[10] The spatial light modulator (SLM) used in the pulse shaper we constructed is a 128-pixel dual-mask device made by Cambridge Research Inc. The SLM has liquid crystal pixels that have a variable index of refraction. The index of refraction changes are due to the voltage across each pixel. This change in the index of refraction introduces a delay to the laser wavelength range in that the pixel can be calculated and controlled. The dual-mask feature of the SLM allows the user to have independent control of the phase and the amplitude of the pulse coming out of the shaper.[11] All of the commands the SLM receives come from the USB port on the side of the device that is connected to a computer. The SLM can be controlled with the stand-alone program for the SLM from the manufacturer, but the SLM in the shaper is mainly controlled using LabVIEW virtual instruments that were written specifically for the shaper. The SLM is able to go from 0 to 10 V with 12-bit precision. It can also retain up to 128 different voltage combinations for the 128 pixels in the SLM.
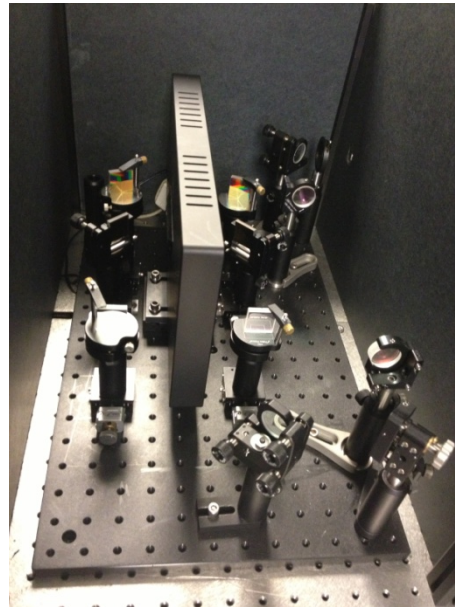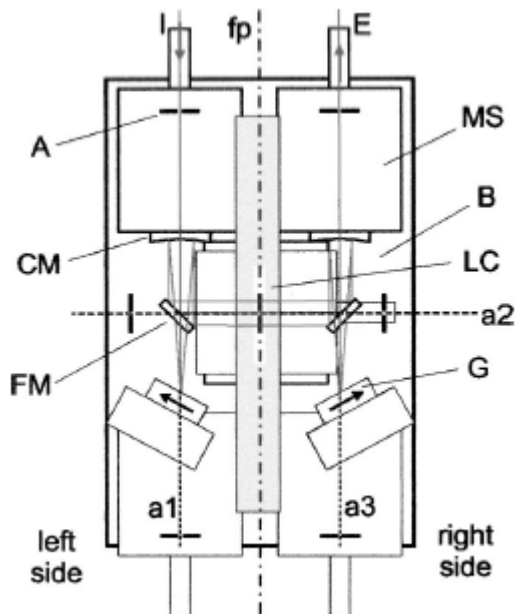
Fig. 5 **(Left) Schematic used to create the pulse shaper we built and (right) the finished product. (Image of the schematic reproduced with permission from Prakelt A, Wollenhaupt M, Assion A, Horn C, Sarpe-Tudoran C, Winter M, Baumert T. Compact, robust, and flexible setup for femtosecond pulse shaping. Rev Sci Instrum. 2003;74(11):4950–4953. Copyright 2003, AIP Publishing LLC. DOI: http://dx.doi.org/10.1063/1.1611998.)**

When designing the pulse shaper, the laser beam must completely fill the face of the SLM. The opening for the SLM is 12.8 mm wide and 5 mm tall, so it becomes necessary to make the laser beam diameter less than 5 mm and spread out to nearly fill the horizontal face of the SLM. Before the laser even encounters the first grating of the shaper, we reduced the beam diameter so the beam would fit through the slit of the SLM using a beam telescope. The beam telescope diameter consists of a 37.5-cm focal length concave mirror and a 15-cm focal length convex mirror. The lengths between these mirrors must be correct in order for the collimated beam to go through the pulse shaper after these mirrors.[12] After the beam diameter was reduced, the beam was directed into the shaper where it first encountered the 1-inch square grating with a blaze angle of 19.71° and a groove frequency of 830.8 grooves/mm. Then, the spatially dispersed beam from the grating was directed into a concave mirror with a focal length of 19.1 cm. We knew that our beam would end up going down, so we put the grating and the concave mirror on stages that allow for horizontal and vertical tilt and rotation along the center axis of the grating. After the concave mirror, the laser beam was directed to the SLM. After the SLM, the arrangement of the second concave mirror and grating is duplicated

to focus the beam back to its original shape and to undo the wavelength separation, respectively. If everything is done correctly, the beam coming out of the shaper should be nearly identical in appearance to the beam coming into the shaper.

We constructed a pulse shaper with all reflective elements, including the beam telescope, to reduce the diameter of the beam. As mentioned previously, lenses can be used to focus the light inside the pulse shapers and prisms to disperse the light inside of the shapers. The lenses are easier to align than the mirrors, and the prisms do not have as much loss as the gratings. However, we did not want to add dispersion onto the laser beam because we were not sure which effects we measured would be from the elements of the shaper and which effects would be from the laser beam. Furthermore, we had worked with another pulse shaper that used a prism to disperse and combine the constituent wavelengths of an ultrafast laser pulse before building this one and discovered that the Poynting vector changed when applying different masks to the laser beam. Parabolic mirrors that focus the beam vertically as well as stop the spread of the beam horizontally can be used. However, this method can increase the peak power density and catastrophically damage the pixels. Instead, we used a concave mirror to stop the horizontal beam dispersion after the grating, which allowed us to shape a more powerful laser beam without damaging the SLM.

When pulse shapers are built with a mirror on the back side of the SLM, it is possible to misalign the beam, causing the incoming beam to have a slightly different path than the outgoing beam and making it simple to pick off the output beam. When using the reflective pulse shaper configuration, one must determine the distances between grating, focusing the mirror and SLM once instead of twice. Additionally, placing a mirror behind the SLM can achieve twice the phase correction of the shaper built at the US Army Research Laboratory. In order to avoid introducing possible alignment errors while building the pulse shaper for the first time, we did not use a mirror. However, these options are under consideration for the design of future versions of this device.

The easiest way to align the pulse shaper is to use the laser beam that will be shaped, without the SLM. A mirror that reflected a level beam back on itself was put in place of the SLM. The grating is placed a distance corresponding to the focal length away from the curved mirror. Then, the SLM mirror is placed that same distance away from the curved mirror. We used an IR viewer to make sure the reflected beam from the mirror put in place of the SLM is reflecting exactly along the path of the incident beam coming into the shaper. Afterward, an ultrafast thin beam splitter is placed into the system after the diameter of the laser beam is reduced; this is done to monitor the beam after it goes through the setup. The beam coming from the beam splitter can then be monitored by a photodiode and an oscilloscope.

The position of the SLM was fixed due to the geometry we had chosen when building the device, so the position of the mirror representing the SLM was fixed as well. This forced us to ensure that the chirp was minimized first. We made sure that the beam was not temporally chirped by putting the beam that had gone through the system into a 10-µm-thick barium borate type-1 crystal and maximizing the SHG signal by changing the distance between the curved mirror and the mirror representing the SLM. Once that length was determined, we worked on the distance between the grating and the curved mirror to make sure the beam was truly collimated. We then ensured that the beams were lying on top of one another because moving the optics to maximize the second harmonic signal or collimation may misalign the beam. This process was continued iteratively until the beam was collimated with no temporal chirp that completely reflected on itself while on the gratings and mirrors in the shaper.

To be sure that everything was working as it should, the laser light that was previously going into the photodiode was sent into the GRENOUILLE; this was done to ensure that the pulse characteristics are the same before and after the shaper apparatus. Once the optimal lengths for the curved mirror and the grating were determined, they were duplicated on the other side of the SLM. The easiest way to make sure everything was working well was to move the GRENOUILLE and measure the pulse characteristics before and after the shaper. To avoid spatial chirp, we used a card to slowly block one side of the beam. If the beam dimmed uniformly, there was no noticeable spatial chirp. If the beam dimmed on one side in a different manner than it did on the other, there was spatial chirp that must be removed before the pulse shaper could be considered complete.

Correct alignment through the shaper is critical and requires tremendous precision. The length between the 2 mirrors used to reduce the diameter should be the difference between the 2 focal distances of the laser, 22.5 cm. Furthermore, the beam should be level throughout this 2-mirror arrangement to avoid spherical aberration and other spatial beam concerns. Once the correct distance is obtained and the beam is level through the arrangement, the beam is allowed to travel across the room and back to verify that it is collimated and level. It is important to have the correct length between the grating and the curved mirror and between the curved mirror and the SLM because an incorrect grating–curved mirror distance will chirp the output pulse while an incorrect curved mirror–SLM mirror distance will prevent the output beam from being collimated. All of the laser beams must be the correct height at all points inside of the shaper. When the beam is not at the correct height through the shaper, errors, including spatial chirp, may occur.

Once the pulse shaper is built and aligned correctly and the SLM is placed back into the pulse shaper, the system needs to be calibrated so that the pulse shaper will

output the correct phase shifts and amplitude outputs. The calibration is done with the laser beam to be shaped, the shaper, and a photodiode that is used to monitor the laser signal strength. We set all of the pixels in mask 2 to the maximum voltage and incremented the voltage of all the pixels of mask 1 slowly from the minimum to maximum voltage settings of the SLM. This was done while measuring and recording the signal strength of the output of the shaper with a photodiode, an oscilloscope, and a LabVIEW program written for this purpose. As the voltage increased for mask 1, we noticed that the laser signal strength had a sinusoidal evolution. The process was repeated, but this time we held mask 1 at the maximum voltage and incremented the voltage of mask 2 in an identical manner to mask 1, and recorded the laser signal strength. Again, we saw a sinusoidal evolution of the laser power. An example of the obtained voltage reading is shown in Fig. 6.
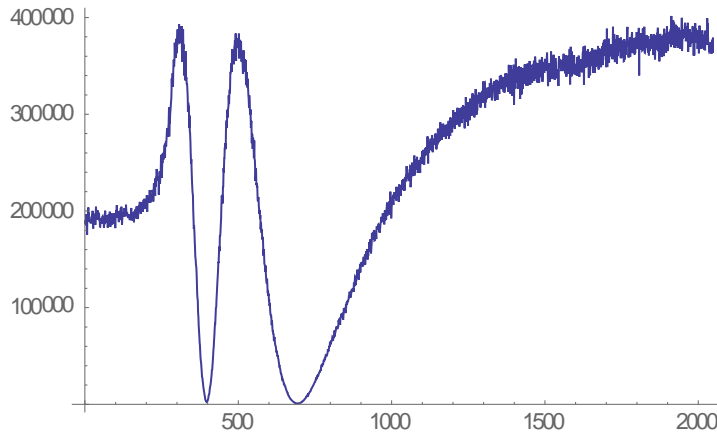

Fig. 6   Initial result for shaper angle calibration

We then took these graphs and converted them into the results found in Fig. 7, where the phase of the pulse shaper goes from almost 0.2 to 4.5π, slightly over 14. Once the phase values corresponding to voltages for masks 1 and 2 are determined, we can calculate the transmission and phase shift of the overall system using the following equations[13]:

$$T = cos^2(\frac{\Phi_A + \Phi_B}{2}) \, . \tag{11}$$

$$\Phi = \frac{\Phi_A + \Phi_B}{2} \, . \tag{12}$$

T is the transmission of the shaper that goes from 0 to 1, or from 0% to 100%, and Φ is the phase of the shaper that ranges as mentioned previously. These 2 equations allow for calculation of Φ_A and Φ_B as a function of transmission and phase of the system.

$$\Phi_A = \Phi + arccos\sqrt{T} \, . \tag{13}$$

$$\Phi_B = \Phi - arccos\sqrt{T} \,. \tag{14}$$

The transmission percentage and the phase of the shaper at a certain pixel are defined by the user. Using these values, one can solve for the phase of each mask, find that in the calibration curve for the specific mask, and set that pixel to the voltage corresponding to that phase shift for each mask.
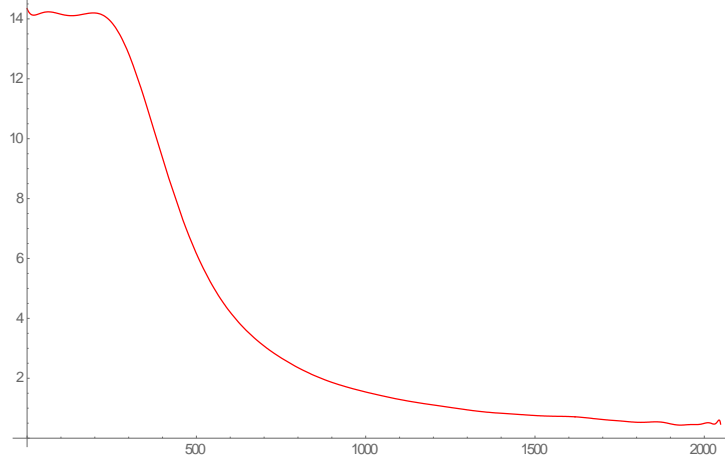

Fig. 7   Final result for shaper angle calibration

The shaper that was constructed is able to handle up to 10% of the beam, which is approximately 300 μJ/pulse. Once the pulse travels through the shaper, the output pulse energy is between 80 and 90 μJ under optimal circumstances. The phase can be shifted between near zero and 4π. The transmission amplitude can be set to between 1% and 100% of the power incident on the SLM.

5.   The Algorithm(s)

Once the shaper was completed, we needed to develop methods to use the shaper to output a transform-limited beam from the pulse shaper. We used 2 different types of algorithms to control the SLM to modify the phase of the laser pulse's constituent wavelengths so that the SHG light from the laser pulse would be optimized, which corresponds to the shortest laser pulse. The first algorithm, a genetic algorithm, was initially used to optimize the pulse width but ultimately was not used as the method of controlling the pulse shaper. We used the second algorithm, the multiphoton intrapulse interference phase scan (MIIPS) algorithm, with the pulse shaper to optimize the laser pulse width.

6. Genetic Algorithm

6.1 Theory

The first algorithm we developed to control the pulse shaper and compress the pulse was a basic genetic algorithm. A genetic algorithm is an evolutionary algorithm based on ideas from biological evolution: reproduction, selection, recombination, and mutation.[14] In general, it works this way: a chosen number of solutions, N, are randomly created that serve to solve a certain problem. This chosen number of solutions is called a generation. After the creation of this first generation, each of these solutions in the generation is evaluated according to a fitness function that is specifically constructed to find an optimal solution to the problem. Afterward, an intermediate generation is selected from the first generation based on the results of the evaluation by the fitness function. To create the second generation of solutions that will be evaluated by the fitness function, the constituents of the intermediate generation are randomly combined with each other to make N new solutions. These new solutions then experience random slight mutations. Once this process is completed, the second generation is ready to be evaluated with the same fitness function that evaluated the first generation. This second generation should score higher with the fitness function than the first generation. This evolutionary process is continued until an optimal solution for the problem is found.[15,16] A flowchart of this idea is shown in Fig. 8.
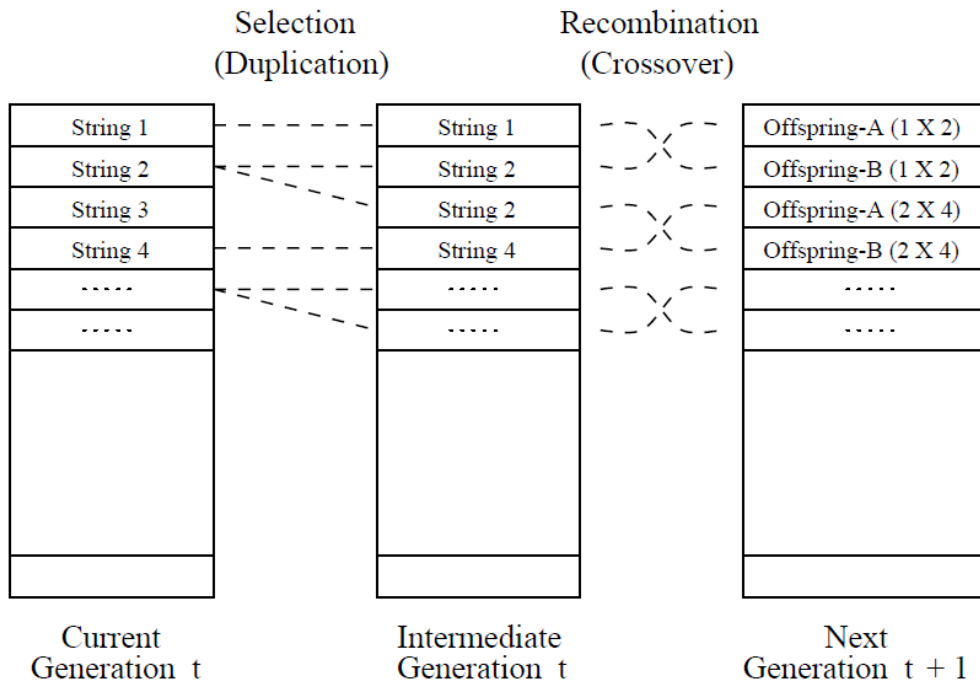

Fig. 8   Flowchart for genetic algorithm

There are many different implementations of each process of this genetic algorithm. A newly created solution can be selected for the intermediate generation using a random selection that is weighted based on its score from the fitness function (rank roulette method or score roulette method) or simply by being in the top half of the best scores (top half method). Mutation methods can vary as well. Elements of a solution in the intermediate generation can be mutated to a random value within the range of possible values (random mutation method), a random mutation value that is more likely to be closer to the original value (Gaussian mutation method), or mutation values that are dependent on the number of generations that the genetic algorithm has done (square root method). Additionally, altering the probability of a mutation or crossover event on a newly formed solutions has an effect on the overall effectiveness of this algorithm. Another common practice when creating a new generation is choosing whether or not any of the solutions making it to the intermediate generation are guaranteed to be in the next generation to be evaluated by creating a small elite population.

6.2 Experiment

We initially tested this genetic algorithm out by solving a classic optimization problem using a genetic algorithm developed using Mathematica. The algorithm would take 30 randomly generated binary numbers (0 and 1) to construct a 30-digit binary number and then use the genetic algorithm to maximize that number. The fitness function used to evaluate each solution was to divide its value by the maximum possible number. We also measured the average score and the highest scoring number for each generation to evaluate the effectiveness of the algorithm and create better solutions as the generations increased. A plot of the evolution of the highest scoring number is seen in Fig. 9.
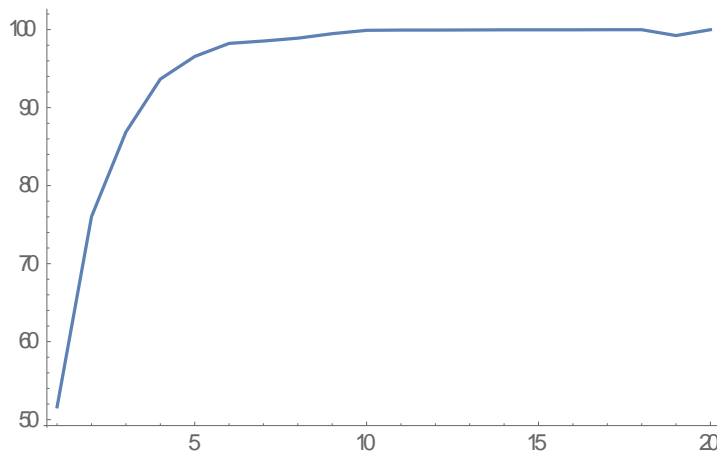

Fig. 9   Output from the sample algorithm in Mathematica

Another test required taking the algorithm over to LabVIEW and duplicating it. However, the problem was changed slightly because the SLM was going to be using 128 pixels and there were approximately 4,000 values that the SLM would accept for voltage. Each solution comprised 128 random numbers between 1 and 4,000, and we wanted all of the numbers in the solution to evolve to 2,000. The fitness function initially was to take the average of all of these points to give an optimal solution to the problem. Then, we changed the fitness function to evaluate each solution based on the average and the standard deviation of the numbers comprising the solutions; the time to arrive at an optimal solution was greatly reduced. This shows the importance of a well-defined fitness function and having more than one evaluation factor in a fitness function.

The work done with this sample algorithm using LabVIEW showed which method, and the strength of that method, was the best choice for each main characteristic of the genetic algorithm to find an optimal solution. The success of the genetic algorithm depends greatly on the number of samples and the selection function. As shown in Figs. 10a and 10b, the algorithm relies on random choices in many respects—more solutions that are being evaluated per generation as well as more generations being evaluated result in more effective solutions. It is possible to use a selection function that is too limiting such that the algorithm does not continue to evolve. It is also possible that an overly strong mutation and crossover setting will negatively affect the evolution. We used the top-half method to determine the best results. This method works by evaluating the solutions—the top half of the solutions are selected for the intermediate generation. The square root mutation technique was used for mutation where the mutations were allowed to be bigger for earlier generations and smaller for higher generations. The mutation probability was kept low between 3% and 5% for reasons shown in Fig. 10c and the crossover probability at 100%.
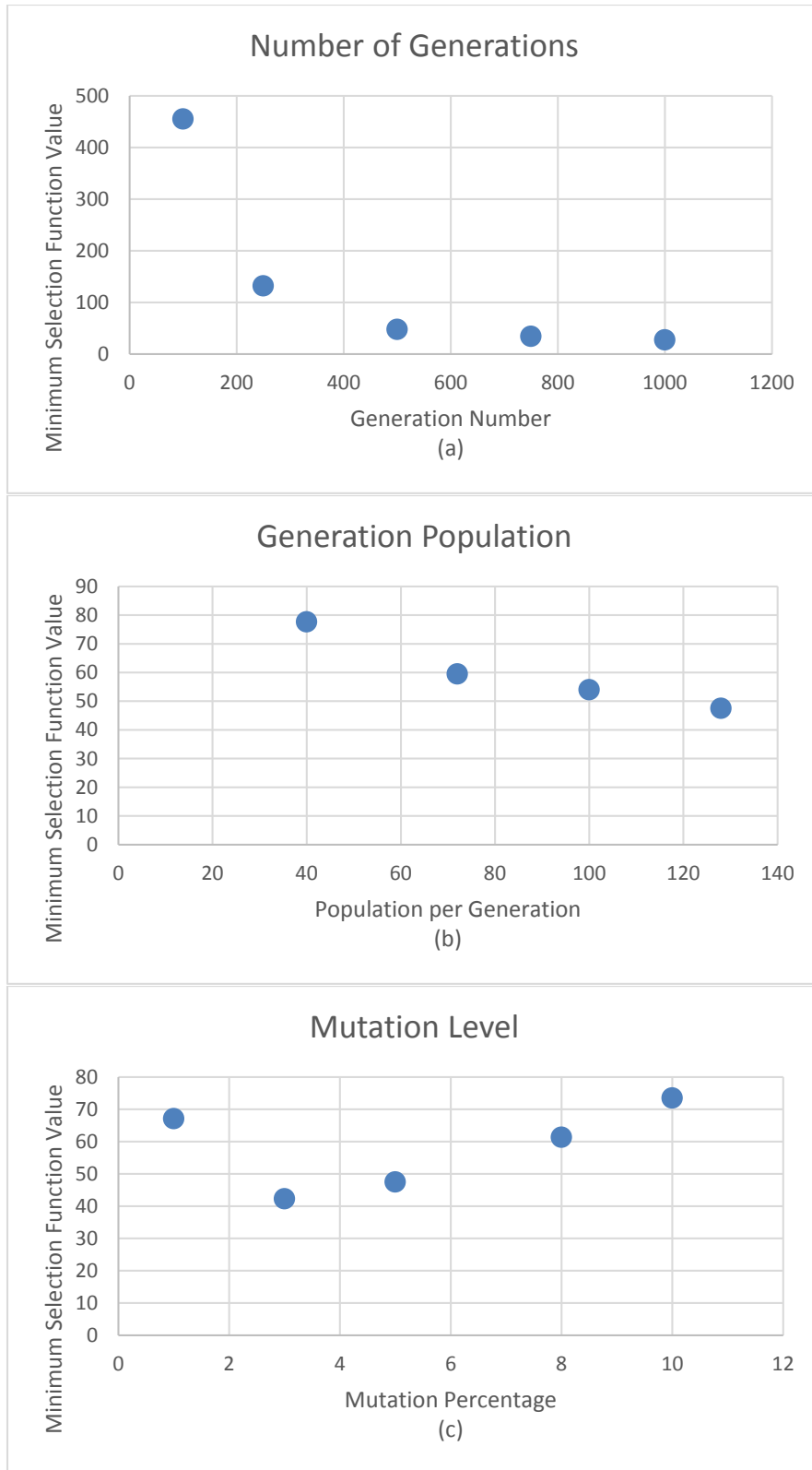
Fig. 10 **Results of test algorithm showing the effect that the a) number of generations, b) population of each generation, and c) mutation percentage has on the ability to determine an optimal solution**

As stated previously, the overall phase and transmission percentage of a pixel in the SLM is related to the phase of each pixel in the 2 masks in the SLM. When using the genetic algorithm with the pulse shaper, each 128 combination of pixels for the 2 masks was a solution. We were doing 100% transmission, so only the phase of each pixel was to be tested with this genetic algorithm. We randomly selected a phase for each pixel of the SLM and collected 128 random phases to generate one solution. This process was repeated for a number of solutions to form a group of solutions that we called a generation. The SLM can retain 128 different combinations of pixel voltages, so we sent the SLM generations that were between 60 and 100 solutions in size. We did not use the complete capacity of the SLM because there were problems with the equipment when using generations that contained 128 solutions. That generation was put into the genetic algorithm to obtain the optimal solution.

One problem with the genetic algorithm is that it is not possible to say for certain whether or not you have the best answer. It is entirely possible to let the algorithm keep going for a better answer. In practice, the algorithm is allowed to run for a certain number of generations or until the evolution of the best answer stops improving at a predetermined rate. There are a number of evolutionary algorithms where a number of solutions are tested against a fitness function and then used to create new solutions that have methods of determining whether or not one has arrived at an optimal solution.

Another problem that plagues evolution algorithms is elitism, which is the process of all the solutions becoming identical. Occasionally, the genetic algorithm stumbles across a solution that scores highly with the fitness function. The solutions from the algorithm are based on that very good solution, and they do not generate better solutions if the solutions are allowed to evolve in another direction. It becomes important to introduce mutations at a certain level to keep the elitism from taking over the evolution of the system. However, the mutation of potential solutions should not be harsh or it will systematically eliminate the best solutions so that the algorithm will never find an optimal solution. We determined that balance in our experiments by altering the level of mutations with our test algorithm, monitoring the results of that test algorithm to determine the best settings and using those settings when doing pulse compression.

Overall, the genetic algorithm is a good tool for finding a solution for the phase to optimize the SHG of the laser beam going through the shaper. Figure 11 shows the evolutionary process of improving the SHG spectrum over approximately 150 generations, and Fig. 12 shows the beginning spectrum and the end result of this 150-generation evolution. However, there are a number of logistical problems with using this technique. The process to complete one generation (create the generation,

put the generation in the SLM, evaluate each solution in the generation, and run calculations for a new generation) takes approximately 1 min. The complete process to obtain Figs. 11 and 12 took over 2 h. Even if we started from an optimal mask previously obtained from an early optimization procedure, we would quickly lose that best answer because of the crossover nature of our algorithm, so there was no way to speed up the process. If the laser output changed in any way, the answer the algorithm had come up with at that time would be useless, and the optimization process would have to be restarted. These overwhelming challenges forced us to find a better way to optimize the phase the shaper introduced to the laser pulse when using a genetic algorithm for SHG optimization.
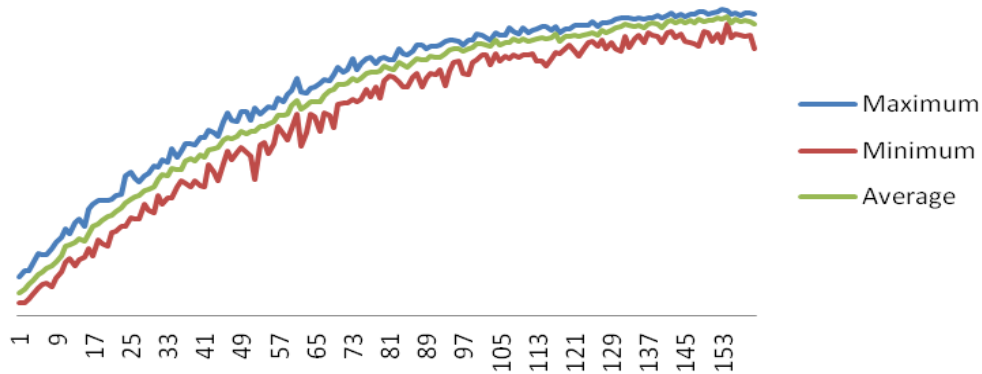
SHG Optimization using GA

Fig. 11   Graph of solution evolution using genetic algorithm on SHG maximization
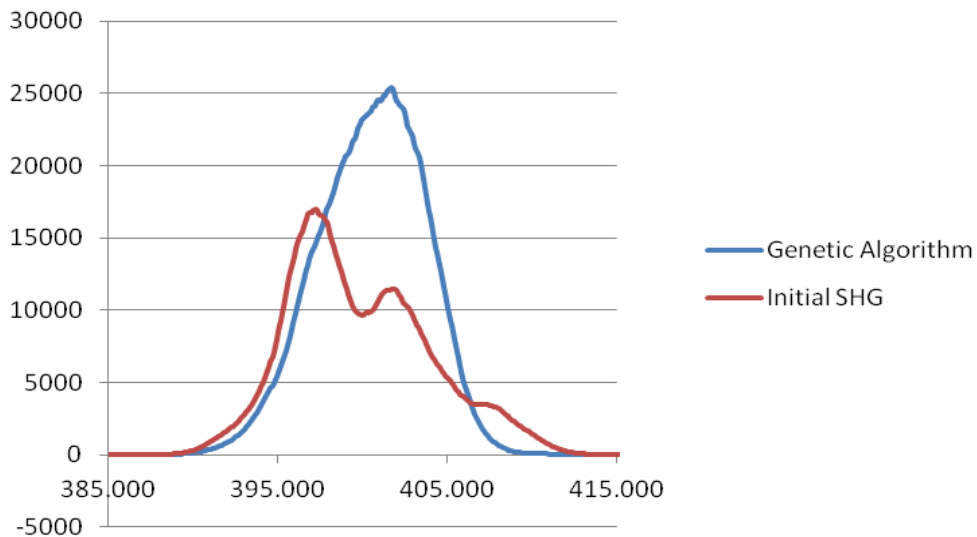
Fig. 12   Before and after result of the SHG maximization using genetic algorithm

19

7.   MIIPS-Based Algorithm

7.1 Theory

The second algorithm we wrote is based on the MIIPS algorithm developed by Marcus Dantus and his team at Michigan State University.[17,18] The MIIPS technique is based on the idea that the second harmonic signal generated by a laser beam is a maximum when the laser beam has a flat phase across all of the wavelengths that comprise a laser beam. As stated previously, the broadband laser pulse can be mathematically expressed as

$$|\epsilon(\omega + \Omega)| \exp[i\phi(\omega + \Omega)],\tag{15}$$

where $|\epsilon(\omega + \Omega)|$ is the amplitude of the pulse, $\exp[i\phi(\omega + \Omega)]$ is the phase of the pulse, and $(\omega + \Omega)$ is the detuning of the pulse due to the pulse's broadband nature. Furthermore, the second harmonic signal, *S(2ω)*, can be written as an integral:

$$S(2\omega) = |\int d\Omega |\epsilon(\omega + \Omega)| |\epsilon(\omega - \Omega)| \exp[i(\varphi(\omega + \Omega))] \exp[i(\varphi(\omega - \Omega))]|^2.\tag{16}$$

According to this equation, the second harmonic would be maximized if the sum of the phases ϕ across all the wavelengths equaled zero. If the detuning of the phases above and below ω was expressed as a Taylor expansion about ω neglecting higher-order terms, we get

$$\varphi(\omega + \Omega) + \varphi(\omega - \Omega) = 2\varphi(\omega) + \varphi''(\omega)\Omega^2 \,.\tag{17}$$

Earlier in this report, a transform-limited beam was defined as a constant or a linear phase. This equation shows that when the second derivative of the phase $\varphi''(\omega) = 0$ is zero, the phase constant and the SHG are maximized because the pulse is transform limited. A reference function $f(\omega)$ is introduced to the pulse shaper to cancel distortions from the spectral phase of the pulse. The total phase the laser pulse will experience, $\varphi(\omega)$, is the sum of the unknown phase $\phi(\omega)$ and the reference phase $f(\omega)$. The same is true for the second derivatives of all of these phases:

$$f''(\omega) + \phi''(\omega) = \varphi''(\omega) = 0 \,.\tag{18}$$

The MIIPS technique for pulse compression uses a pulse shaper to place a series of reference phase patterns on a laser pulse and then monitors the spectrum of the SHG response from those reference phase patterns. This is done to calculate the phase shape of the pulse as a function of wavelength and apply the necessary phase pattern to cancel the phase pattern of the input beam to output a transform-limited pulse from the pulse shaper.

The unknown phase is determined by placing a reference phase on the laser pulse and monitoring the output of the shaper as we modify the phase pattern on the SLM in the shaper. The SHG spectrum has a local maximum at ω when the second-order phase distortion is equal to zero, which means the second derivative of the reference function and the unknown phase function need to equal zero. The reference phase function is $f(\delta, \omega) = \alpha \sin(\gamma\omega - \delta)$, where α is the amplitude of the phase shift, γ is the time duration of the pulse, ω refers to the laser frequency ($\omega = \pi c/\lambda_{SHG}$), and δ is a phase shift from 0 to 4π. As the phase shift δ goes between 0 and 4π in a predetermined number of steps, a spectrum is generated for each step. This collection of spectra is used to generate a hyperspectral image that indicates how close or far the reference spectrum is to the ideal spectrum needed to output a transform limited beam. An ideal hyperspectral image would show that where the reference phase pattern is flat, a maximum value for the SHG signal would be measured. Any deviation from this expected measurement shows that the pulse is not transform limited. A before and after image of the hyperspectral diagram generated by a MIIPS optimization process is seen in Fig. 13.
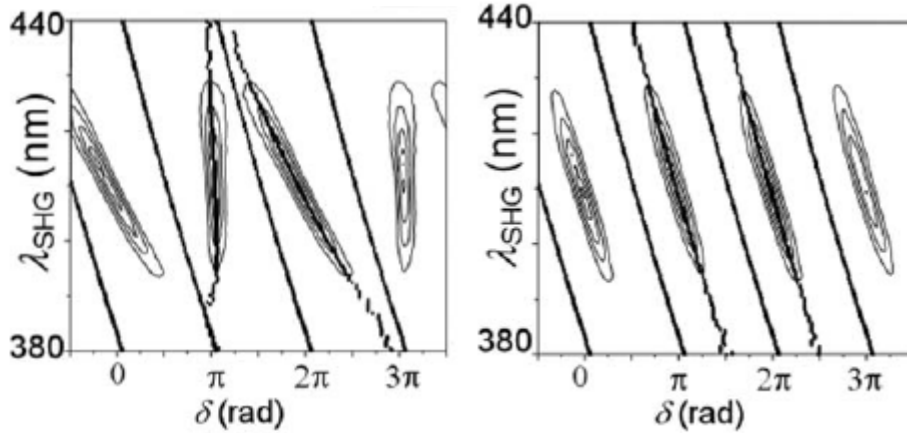

Fig. 13 **Before and after hyperspectral images used to compress pulses using MIIPS[18] (image used with permission)**

7.2 Experiment

When the hyperspectral image is created from the collection of spectra recorded as the reference function went through the phase shifts, phase shifts to the unknown phase function must be calculated to completely determine the phase function of the laser pulse. As the reference phase function undergoes its phase shifts, 5 regions for evaluation in the hyperspectral image are monitored: 0 to $\pi/2$, $\pi/2$ to $3\pi/2$, $3\pi/2$ to $5\pi/2$, $5\pi/2$ to $7\pi/2$, and $7\pi/2$ to 4π. Only the first 2 complete regions, $\pi/2$ to $3\pi/2$ and $3\pi/2$ to $5\pi/2$, are used for analysis. For each of the spectra in those 2 regions, the maximum value for each phase shift is determined. Then, only the maximum

values for the wavelengths that correspond to pixels 53–74 are retained, which is the middle of the SLM where the largest values can be found. Using these 21 points, the maximum value for all 128 pixels on the SLM is estimated using a linear interpolation. Once these maximum values are determined, the second derivative of the unknown phase function is calculated, $\phi''(\omega) = \alpha\gamma^2 \sin[\gamma\omega - \delta_{max}^n(\omega)]$, and the unknown phase function is obtained for each of the 2 observed regions, and the average is taken to calculate $\phi(\omega)$. The newly obtained unknown phase factor $\phi(\omega)$ that was calculated is now added to the initial reference function and a new generation is created. The phase shifts are then added to the new reference phase function to create 64 new reference phase functions for the 64 phase shifts and the process is repeated again. As this process is repeated, the calculated phase shifts that are added to the reference phase function get smaller and smaller. This optimization process normally takes 4–5 generations. The hyperspectral diagram before and after the MIIPS-based algorithm on the laser beam is shown in Fig. 14.
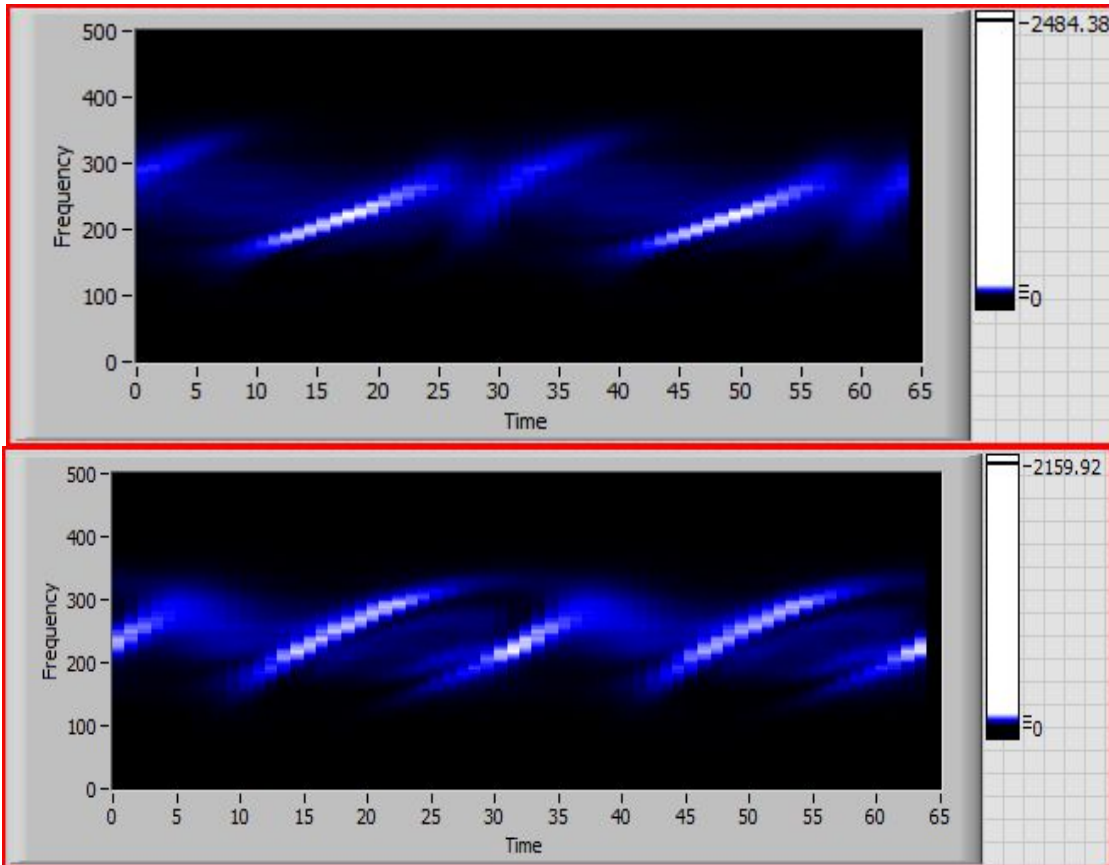

Fig. 14   Before and after hyperspectral images from the MIIPS algorithm

The MIIPS algorithm is better for determining a transform-limited beam than the genetic algorithm. First, there is a definitive way to know how close the reference phase function is to the needed phase function to generate a transform-limited pulse coming out of the pulse shaper. Second, the MIIPS algorithm is much faster than the genetic algorithm. The MIIPS algorithm can generate a pulse that is very nearly transform limited in 5 generations, and the optimization process can take less than 5 min. Ultimately, the MIIPS algorithm achieves better results than the genetic algorithm when optimizing an SHG, as seen in Fig. 15.
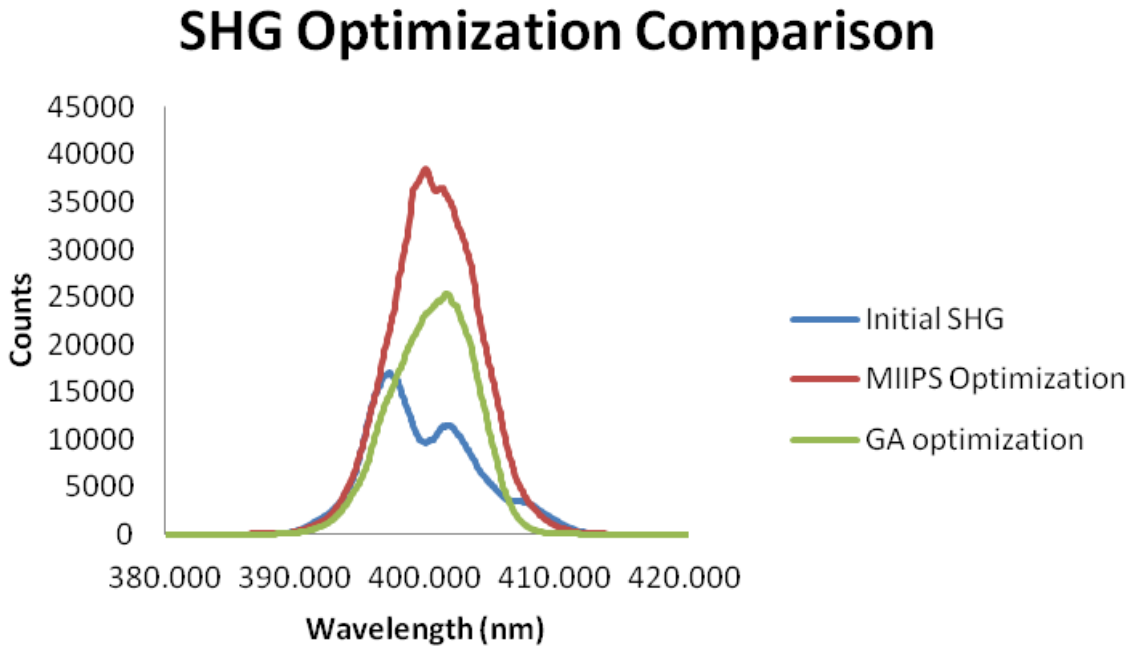

Fig. 15   SHG optimization comparison between genetic algorithm and the MIIPS algorithm

8.   Summary and Conclusion

We have constructed 2 different types of pulse compression devices and developed 2 different algorithms that are used to temporally optimize femtosecond laser pulses. The first device, a prism compressor, was used to statically compress broadband white light pulses using the geometry of the prism to eliminate second-order dispersion. The second type of device, an SLM-based 4*f* Fourier transform pulse shaper, was an improvement on the prism-based pulse compressor because of its ability to dynamically handle higher-order dispersion of the output pulse from the laser system. The genetic algorithm used with the SLM-based pulse shaper allows users to optimize any process for which an effective selection function can be determined. The MIIPS algorithm in use with the SLM-based pulse shaper allows the user to quickly optimize the beam because of linear and nonlinear dispersions.

9.   References and Notes

1. Weiner AM. Ultrafast optics. Hoboken (NJ): John Wiley and Sons; 2009.

2. Rullière C. Femtosecond laser pulses: principles and experiments. New York (NY): Springer; 2005. p. 426.

3. Trebino R. Frequency-resolved optical grating: the measurement of ultrashort laser pulses. Norwell (MA): Kluwer Academic Publishers; 2000. p. 425.

4. GRENOUILLE = grating-eliminated no-nonsense observation of ultrafast incident laser light e-fields.

5. Boyd RW. Nonlinear optics. Boston (MA): Academic Press; 2008.

6. Diels J. Ultrashort laser pulse phenomena: fundamentals, techniques, and applications on a femtosecond time scale. Boston (MA): Elsevier/Academic Press; 2006.

7. Akturk S, Gu X, Kimmel M, Trebino R. Extremely simple single-prism ultrashort-pulse compressor. Opt Express. 2006;14(21):10101–10108.

8. Brady JJ, Farrell ME, Pellegrino PM. Discrimination of chemical warfare simulants via multiplex coherent anti-Stokes Raman scattering and multivariate statistical analysis. Optical Engineering. 2013;53(2):021105–021105.

9. Vaughan JC. Ultrafast pulse shaping. In: Trebino R, editor. Ultrafast optics; 2008 [accessed 2016 Mar 4]. http://www.frog.gatech.edu/prose.html.

10. Prakelt A, Wollenhaupt M, Assion A, Horn C, Sarpe-Tudoran C, Winter M, Baumert T. Compact, robust, and flexible setup for femtosecond pulse shaping. Rev Sci Instrum. 2003;74(11):4950–4953.

11. Zhang Y, Wu LY, Zhang J. Study on the phase modulation characteristics of liquid crystal spatial light modulator. Journal of Physics: Conference Series. 2006;48(1):790.

12. Palmer C, Loewen E. Diffraction grating handbook. Irvine (CA): Newport Corporation; 2005. p. 271.

13. Jiang Z. Reflective pulse shaper design and implementation with high resolution/low loss. West Lafayette (IN): Ultrafast Optics and Optical Fiber Communications Laboratory, Purdue University; 2004.

14. Sadjadi F. Comparison of fitness scaling functions in genetic algorithms with applications to optical processing. Proc SPIE 5557, Optical Information Systems II. 2004;5557:356.

15. Ashlock D. Evolutionary computation for modeling and optimization. New York (NY): Springer-Verlag; 2004.

16. Whitley D. A genetic algorithm tutorial. Statistics and Computing. 1994;4(2):65–85.

17. Xu B, Gunn JM, Cruz JMD, Lozovoy VV, Dantus M. Quantitative investigation of the multiphoton intrapulse interference phase scan method for simultaneous phase measurement and compensation of femtosecond laser pulses. J Opt Soc Am B. 2006;23(4):750–759.

18. Lozovoy VV, Pastirk I, Dantus M. Multiphoton intrapulse interference. IV. Ultrashort laserpulse spectral phase characterization and compensation. Opt Lett. 2004;29(7):775–777.

List of Symbols, Abbreviations, and Acronyms

GVD	group velocity dispersion
MCARS	multiplex coherent anti-Stokes Raman spectroscopy
MIIPS	multiphoton intrapulse interference phase scan
SHG	second harmonic generation
SLM	spatial light modulator

INTENTIONALLY LEFT BLANK.